INJURY BIOMECHANICS RESEARCH
Proceedings of the Twelfth International Workshop

OCCUPANT INTERACTION WITH THE STEERING SYSTEM

P.C. Begeman, Wayne State University

INTRODUCTION

Field accident data indicate that the steering wheel rim is severely bent in many fatalities of unrestrained drivers. This phenomenon was not observed consistently in laboratory tests in which a variety of surrogates were used to simulate these field accidents. The steering wheel is the component of the steering system contacted by the upper body in automotive crashes; and load distribution on the occupant is likely to be influenced by the location and shape of the steering wheel and the construction of the wheel. Also, steering wheel deformation is dependent on occupant load distribution on the wheel. In order to establish the suitability of various mechanical surrogates for the assessment of thoracic (and abdominal) injuries, human cadavers were used to study their effect on the steering system and their ability to duplicate accident observations.* That is, field accident severity was considered duplicated if similar steering wheel deformations were obtained using cadavers. Although human cadavers have significant limitations in simulating accident victims, they can be used effectively in the evaluation of steering system response. That is, the analysis will be focussed more on steering wheel deformation and less on the injury pattern of the surrogate. In this way, some of the limitations of human cadavers as a test surrogate can be reduced.

---

*The rationale and experimental protocol for use of human cadaver research subjects in this program have been reviewed by the General Motors Research Laboratories Human Research Committee and The Human Investigation Committee of Wayne State University. The research complied with the provisions of the Uniform Anatomical Gift Act, followed guidelines established by the U. S. Department of Transportation, National Highway Traffic Safety Administration and recommendations of the National Research Council of the National Academy of Sciences, and adhered to the provisions of the Declaration of Helsinki.

This research consisted of a series of sled tests using a non-production, non-collapsible steering system in a fixed position with identical steering wheels; wheel parameters were not considered in these tests. Part 572 and Hybrib III dummies were also run in identical test conditions as the cadavers for comparison of responses. Injury patterns and responses in the cadavers were also noted.

METHODS OF PROCEDURE

The test subjects were run on the WHAM III sled in a test fixture consisting of a hard seat and seat back, a steering column and wheel mounted to a rigid frame through a triaxial load cell at an angle of 15 degrees with respect to a horizontal plane, and a padded head stop. Figure 1 shows the test setup. Knee restraints were also mounted on the frame and were covered with 100 mm of styrofoam. This arrangement was not made to simulate any particular automotive interior. A uniaxial load cell was placed in the center of the steering wheel to measure hub loads. Subtracting the hub load from the total column load as measured by the triaxial load cell gives the wheel rim and spoke load. Occupant instrumentation consisted of triaxial accelerometer in the head and chest of the anthropomorphic dummies and for cadavers a nine accelerometer cluster was used on the head, a triaxial accelerometer on T1 and a pressure transducer in the aorta. Photographic targets were attached to the spinous process of T1, T8 and T12 by means of bone screws. Other targets were attached to various locations of the head and torso. Chest deformations were measured photographically using the T8 target on the spine and a column target starting at the time of contact of the chest with the hub. Fuji Prescale film was taped around the steering wheel rim and hub to sense peak contact steering wheel and hub pressures. The height of the occupants were adjusted so that the top of the steering wheel was approximately at the level of T1.

The sled was accelerated slowly to approximately 37 or 42 km/h and then stopped over a distance of 305 mm by a hydraulic snubber. By positioning the subjects approximately 381 mm from any potential impact surface (wheel or knee restraints) the sled came to a complete stop before the subject was in contact with any vehicular surface. This made the analysis of data easier and rendered the velocity of occupant impact approximately equal to the sled velocity. This change in velocity, of 37 to 42 km/h, simulated a fairly severe accident. Three high cameras recorded the kinematics, one on-board and the other two off-board in lateral and overhead positions. Cadavers were subject to pre-run x-ray qualification and post-run autopsy to determine the detailed extent of injuries. This series of tests consisted of four runs using unembalmed cadavers, two with the Part 572 dummy and three with the Hybrid III dummy.

RESULTS

Figure 1 shows, the wheel deformation after a dummy impact. In no dummy tests did the wheel rim deformation exceed 51 mm which was approximately the level of the hub. From Figure 2, the wheel deformation from a 42 km/h cadaver run can be seen. The rim deformed 110 mm, well past the hub. Figure 3 shows the wheel deformation from a fatal accident. It appeared that the field accident deformation was still slightly higher but, it was decided that 42 km/h was sufficient to study occupant interactions. Dummy chests bottomed out at both 37 and 42 km/h while cadavers only showed evidence of bottoming at 42 km/h. Figures 4 and 5 show the column and hub loads for a dummy and a cadaver run at 37 km/h, respectively. The column loads and the hub loads were considerably higher and of shorter duration for dummies, approximately 45 ms versus 65 ms for cadavers. Note the end of the sled acceleration and inertial forces before occupant contact with

the wheel. Figures 6 and 7 show the column and hub loads for 42 km/h dummy and the cadaver runs, respectively. Again, the dummy loaded the hub and column more severely. The loads in both cases were significantly higher than those for the 37 km/h run. The sharp rise in the load traces were indicative of a bottoming out phenomenon. Since the higher velocity runs are of more interest, discussion will concentrate on those runs.

Table 1 lists the cadaver data. All suffered multiple rib fractures which could result in a flail chest in a living subject and most also had neck injuries which resulted in the high AIS number. No abdominal or soft tissue injuries were found in any of the cadavers. Table 2 lists the peak data. Loads were not been normalized. Comparing the x-axis column load and hub loads for dummies against cadavers it can be seen that cadaver loads were approximately half those of the dummies. Also tabulated are the rim loads, which were higher in magnitude for dummy runs, primarily because the total dummy loads were much higher. It is interesting to note that cadaver rim loads seemed to be limited to approximately 5000 N. This could be a property of the wheel. These rim loads were calculated at the time of the peak column and hub load. The percent rim load data at the time of peak show a different trend. In general the cadaver percentages were higher than those of the dummy. These percentages were not constant but were a function of time. They differed between dummies and cadavers. Percentage rim loads as a function of time for a dummy is shown in Figure 8. There is a high percentage at first contact followed by a sharp drop to a low percentage occurring around the time of the peak loading. As the occupant rebounds, the hub is unloaded first, and since the rim was not deformed past the hub, there is high rim load percentage at the end. Figure 9 shows the percent rim loads for a cadaver run. They started out

in the same manner but, since the rim was deformed past the hub it unloaded first and the percentage rim load dropped to zero. From these two figures it can also be seen that the wheel contact time for the dummy was shorter. Actual rim loads versus time are shown in Figures 10 and 11. The drop in the cadaver rim loads, shown in Figure 11, at approximately 190 ms could be due to rim "snap-through". The higher rim loads in the dummy run must be mostly distributed on the spokes near the hub since the rim did not "snap-through." Fuji film was not read for pressure but, in general it showed a much more uniform load distribution over the whole wheel for cadavers while dummies generated local spots of contact pressure.

Chest deformations for the 37 km/h runs were not significantly different between the cadavers and Hybrid III. However, at 42 km/h they were. Wheel deformations likewise showed the most significant differences at the higher velocity. Also tabulated are several different injury parameters. The data here were too limited to make any comparisons between runs. However, they were used to compute several parameters. The Nor(V) + Nor(C) is the sum of the normalized peak chest velocity peak chest deflection divided by chest depth. V*C is maximum of the product of chest velocity and relative chest deflection divided by the chest depth.

Chest deflection for a cadaver is shown in Figure 12 and for the same velocity (42 km/h) run that of a dummy is shown in Figure 13. Besides Chest deflection was less for the dummy and its duration was shorter. In these runs the rebound velocity of the dummy was greater than that of the cadaver. This would indicate that the cadaver chest was absorbing more energy than the dummy. No doubt the fracturing of the ribs contributed to this absorption of energy. One of the reasons for the high column loads in

dummy runs is due to the chest bottoming out. This shows up clearly in the force-deflection plots of the chest, such as in Figure 14. There was a short period of high rate of loading followed by a long period of approximately constant load during which the chest was compressed and ending with a high load spike when the chest bottomed out. Force-deflection curves for a cadaver were somewhat different, as shown in Figure 15. The high load spike at the end of the pulse is missing and the hysteresis loop is larger. There was however, a rise at the end of the 42 k m/h run indicating that the cadaver chest also bottomed out. This rise was not as evident in the 37 km/h cadaver runs. It should also be noted that the bending of cadaver during impact, also participated in the absorption of energy. This did not occur in dummies.

One popular model of the chest is the Lobdell model (1), shown in Figure 16. This model is primarily used for pendulum impact, where M1 is the pendulum mass, M2 is the sternum, and M3 is the spine and other organs. M2 and M3 are initially at rest and M1 is the velocity of the pendulum. For this application M1 was started at rest and given a very large mass to simulate a fixed steering column, while M2 and M3 were given initial velocities of -42km/h. Spring and damper values used were Lobdell's original data as listed in the Figure 16. Results are shown in Figure 17. They follow the test data well in the beginning but lacked the bottoming out stiffness change. An attempt was made to simulate the bottoming out phenomenon by adding an additional spring to the models. The results did not suitably match the test data. However, by adding an additional damper (4 in/lbs/sec) at 80 mm the model results matched the test data very well, as seen from Figure 18. Thus, the bottoming out of cadaver chests is more of a hydraulic action than that of a linear spring. Lobdell's model was also run for dummy data as originally determined by Lobdell. The results

are similar to the cadaver situation in which the bottoming mechanism is missing. By providing an additional spring (4500 lbs/in) at 85 mm, the results shown in Figure 19 were optained. The results were very good up to the end where the peak load was somewhat lower and some hysteresis is lacking. Modifications to the valves of M3 and damping should further improve the results. Support for the hydraulic hypothesis for cadavers can be found from Figure 20 which is a plot of aortic pressure against chest deflection. There was essentially no pressure until the chest was almost bottomed out at which time the pressure rose rapidly.

DISCUSSION

Since the cadaver has a more compliant chest it deforms the steering wheel rim and allows the steering column to penetrate the chest, which may increasing the liklelihood of rib fractures. If the steering wheel was stiffer the load would be distributed over a larger area and the injury potential could be lessened. Also, the dummy chest was too stiff in the frontal plane and did not allow itself to be wrapped around the column. The dummy chest also does not have enough room for the deflection required.

CONCLUSIONS

It is clear from this study that dummies cannot simulate wheel deformations properly at high severity impacts, as the frontal area is too stiff. their chests do not seem to be able to absorb sufficient energy to simulate realistic rebound kinematics. Articulation in the spine would be helpful also. Bottoming out of the dummy chest led to excessively high column loads. Based on test force deflection data, Lobdell's model could simulate the results fairly well if provisions were made for a bottoming out spring of sufficient stiffness. This should be of the hydraulic type for cadavers and linear spring type for dummies.

ACKNOWLEDGEMENT

This research was sponsored in part by the Biomedical Science Department of General Motors Corporation.

REFERENCES

1. Lobdell, "Impact Response of Human Thorax", in Human Impact Response ed. by King, W. and Mertz, H., pp 225-243, Plenum Press, NY, 1973.

TABLE 1

Relevant Cadaveric Anthropometric and Injury Data

Run No.	Cad. No.	Age/ Sex	Weight (kg)	Chest depth (mm)	Cause of death	Injury Summary	AIS
4	238	59M	49	180	Methane gas	Fx ribs 3-6 Fx C4, Sep Hd/C1	6
5	200	57M	64	210	MI	Flail chest Sep C5/C6	5
9	277	66M	86	280	MI	Flail chest	2
10	274	57F	70	230	MI	Flail chest Fx T1, sep T1/T2	4

TABLE 2

Peak Data Summary

Run	3	4	5	6	7	8	9	10	11
Occ	Pt572	C238	C200	Hyb3	Hyb3	Pt572	C277	C274	Hyb3
Vel (KM/H)	37.8	37.9	36.7	39.8	38.9	42.2	41.4	42.2	42.8
Colx(N)	17500	8500	7200	19250	21000	19000	13000	12500	29000
Coly(N)	-1130	1010	-1980	-2000	2100	3800	1500	1100	5600
Colz(N)	-2600	-2300	-1400	-3500	-3400	-5600	-2500	-4000	-10000
Hub(N)	8750	3550	2250	11500	8500	10700	7800	7500	24000
Rim(N)	8750	5000	5000	7800	12500	8300	5200	5000	5000
Rim(%)	50	59	69	40	60	44	40	40	17
Headx(G)	-111	-240	-111	-60	-72	-	-250	-220	-100
Heady(G)	4	15	20	5	-8	-	-28	27	5
Headz(G)	54	135	50	120	49	-	100	100	120
HIC(S)	1048	6631	1226	1087	613	-	3196	1493	1204
Chestx(G)	-57	-64*	-45*	-71	-71	-	-30*	-60*	-88
Chesty(G)	-19	-35*	30*	4	-9	-	-18*	22*	21
Chestz(G)	23	98*	-*	21	31	-	55*	28*	45
GSI(S)	327	918*	171*	470	441	-	-*	392*	814
3MS(G)	60	91*	38*	72	68	-	-*	53*	94
CHDf(MM)	60	98	94	100	88	-	128	124	93
No(v)+No(C)	0.85	1.03	0.88	1.32	1.31	-	1.06	1.15	1.23
V*C(M/S)	0.17	2.31	1.55	1.61	1.40	-	1.18	2.18	1.11
VasPr(KPA)	-	65	-	-	-	-	-	85+	-
WhDf(MM)	17	51	33	39	43	19	114	109	51
Spoke	hor	hor	hor	hor	ver	hor	hor	hor	ver

* Accelerations not at the same location as dummy (T1 vs T8)
+ Signal saturated

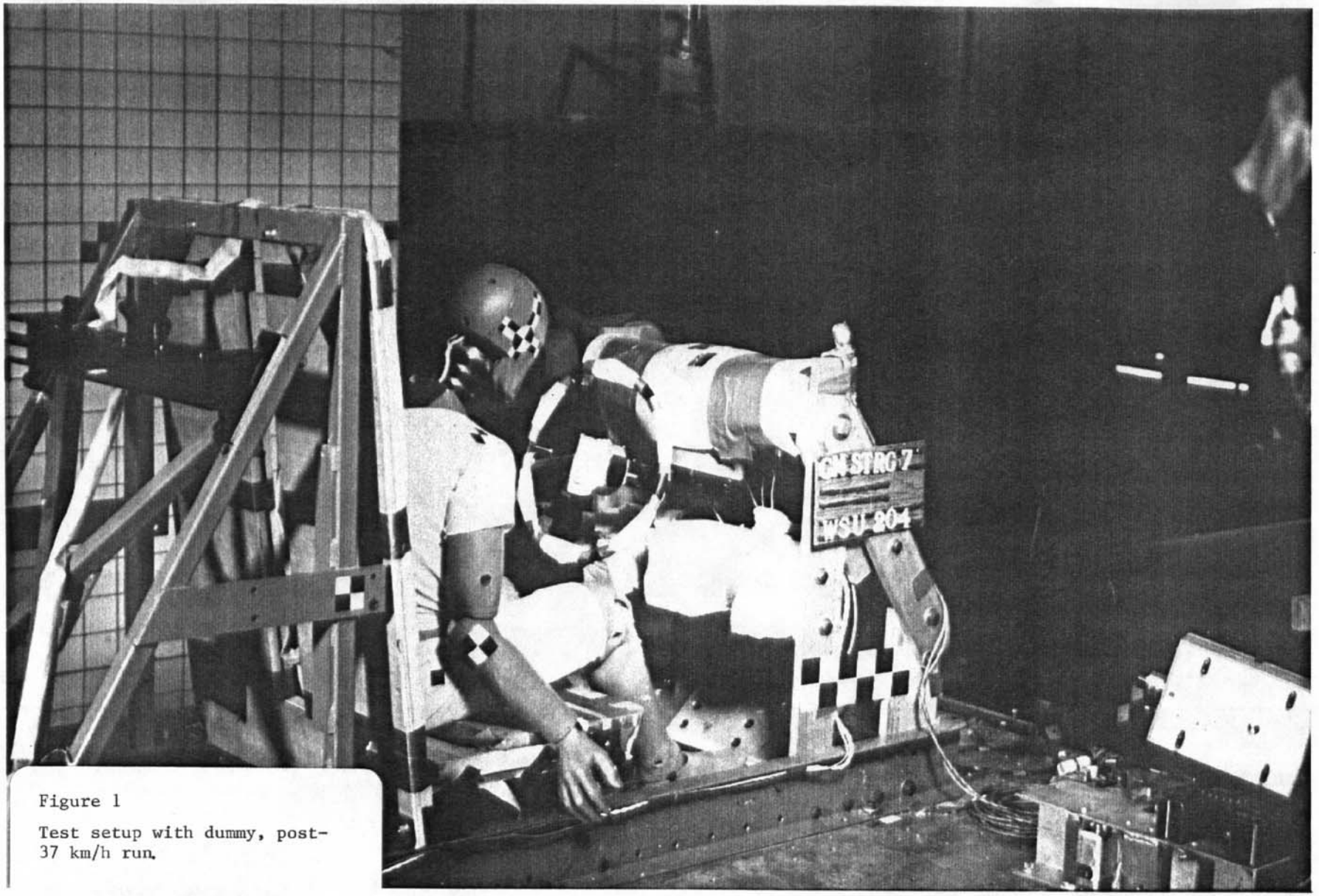

Figure 1

Test setup with dummy, post-37 km/h run.

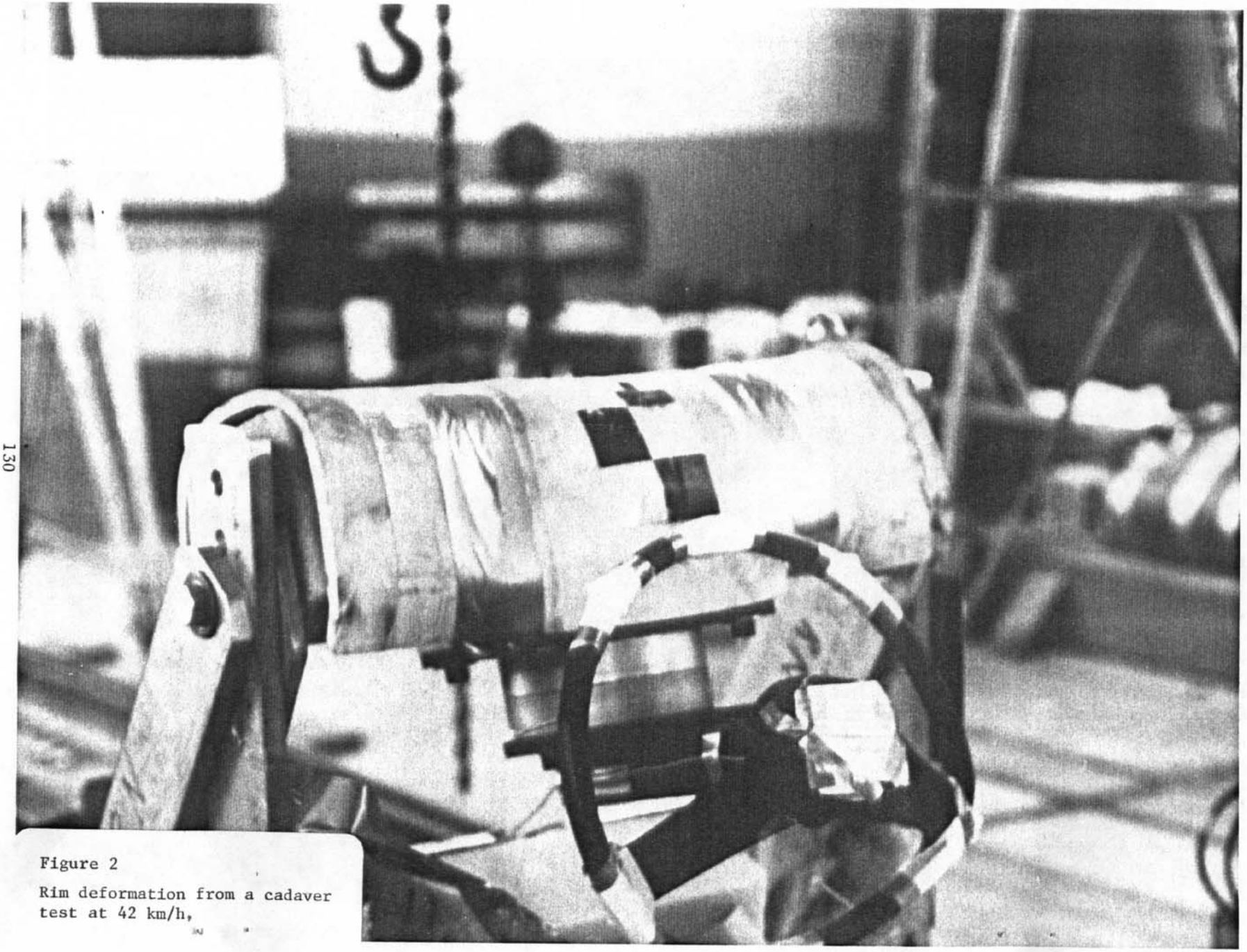

Figure 2

Rim deformation from a cadaver test at 42 km/h,

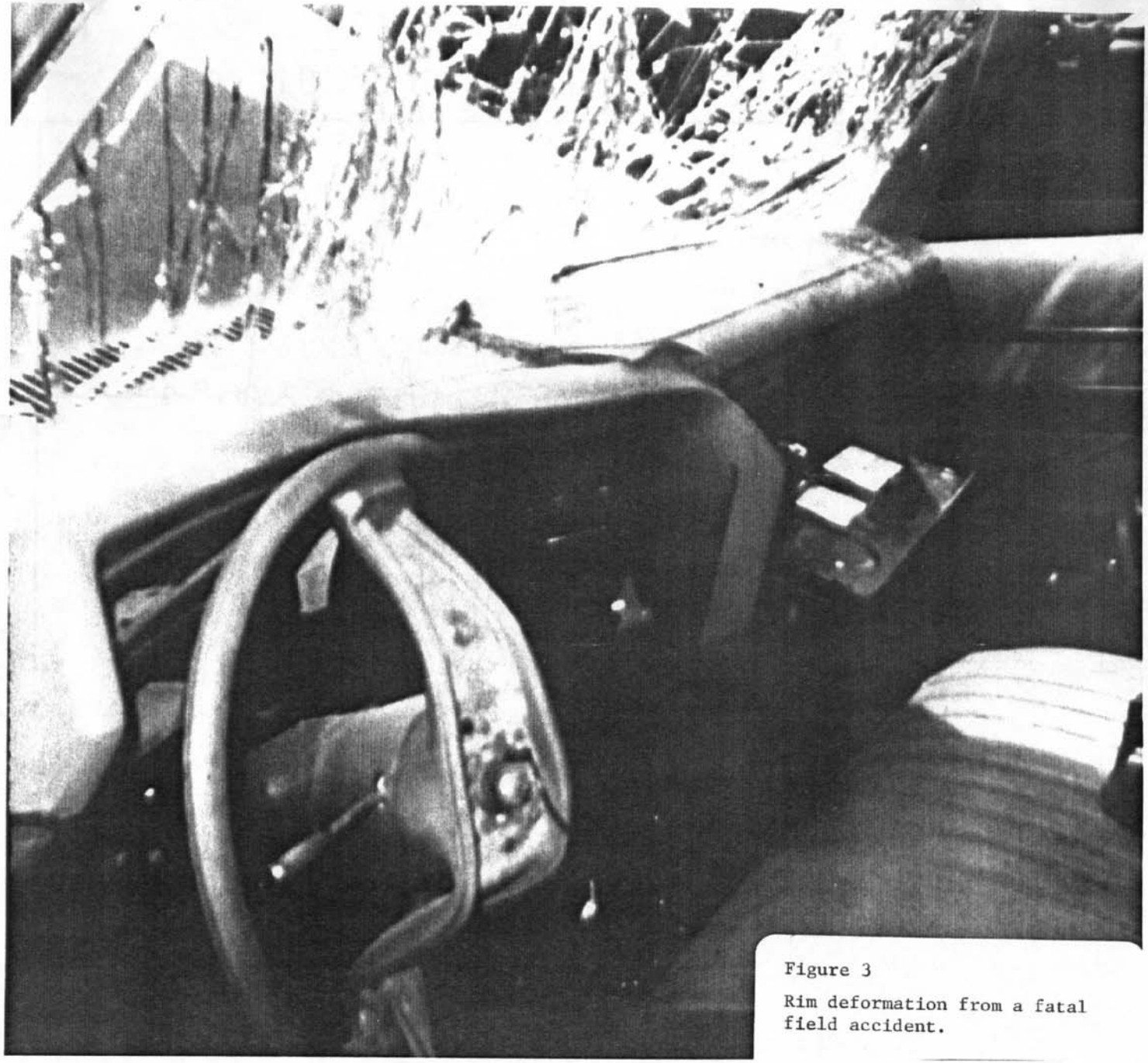

Figure 3

Rim deformation from a fatal field accident.

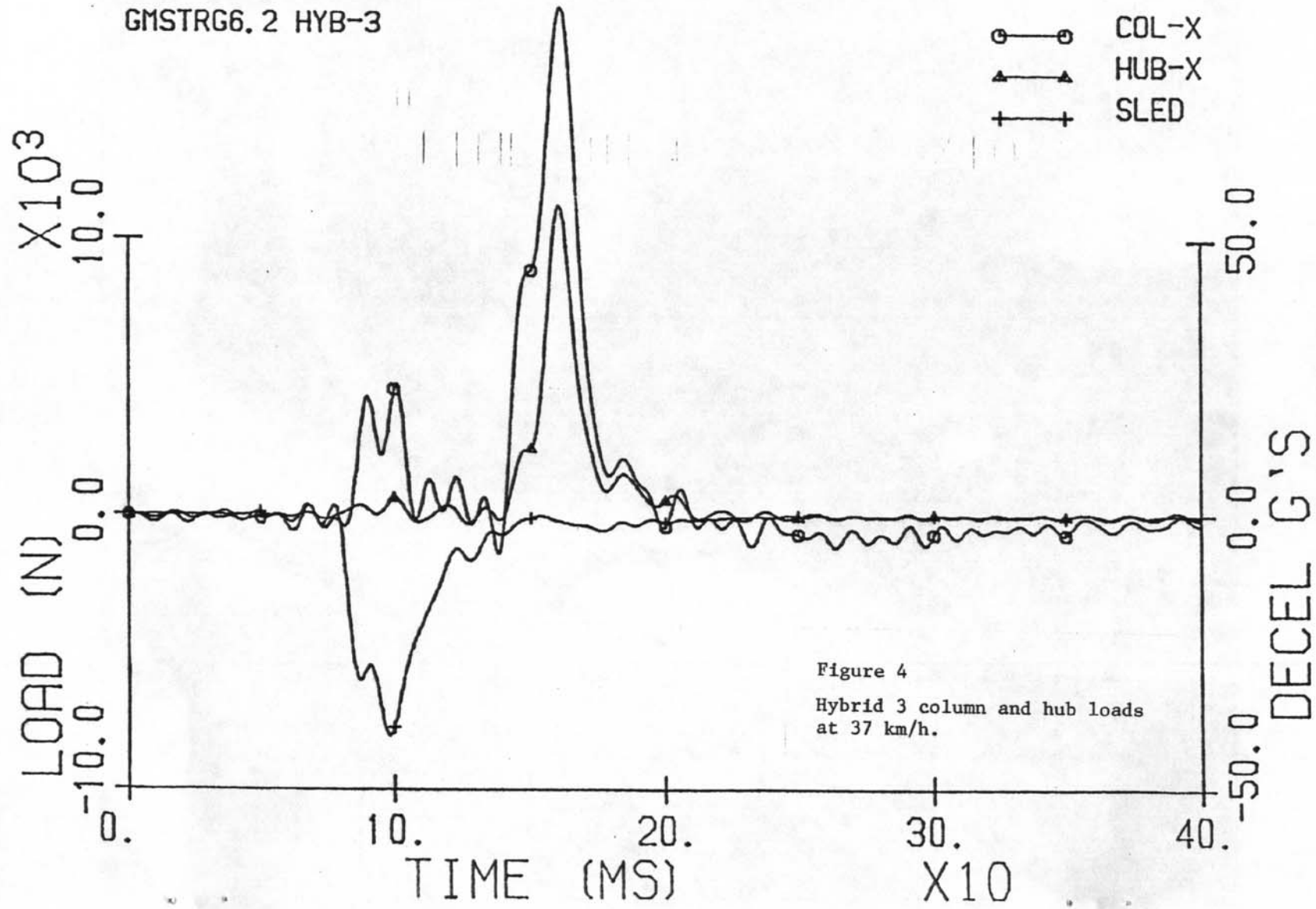

Figure 4

Hybrid 3 column and hub loads at 37 km/h.

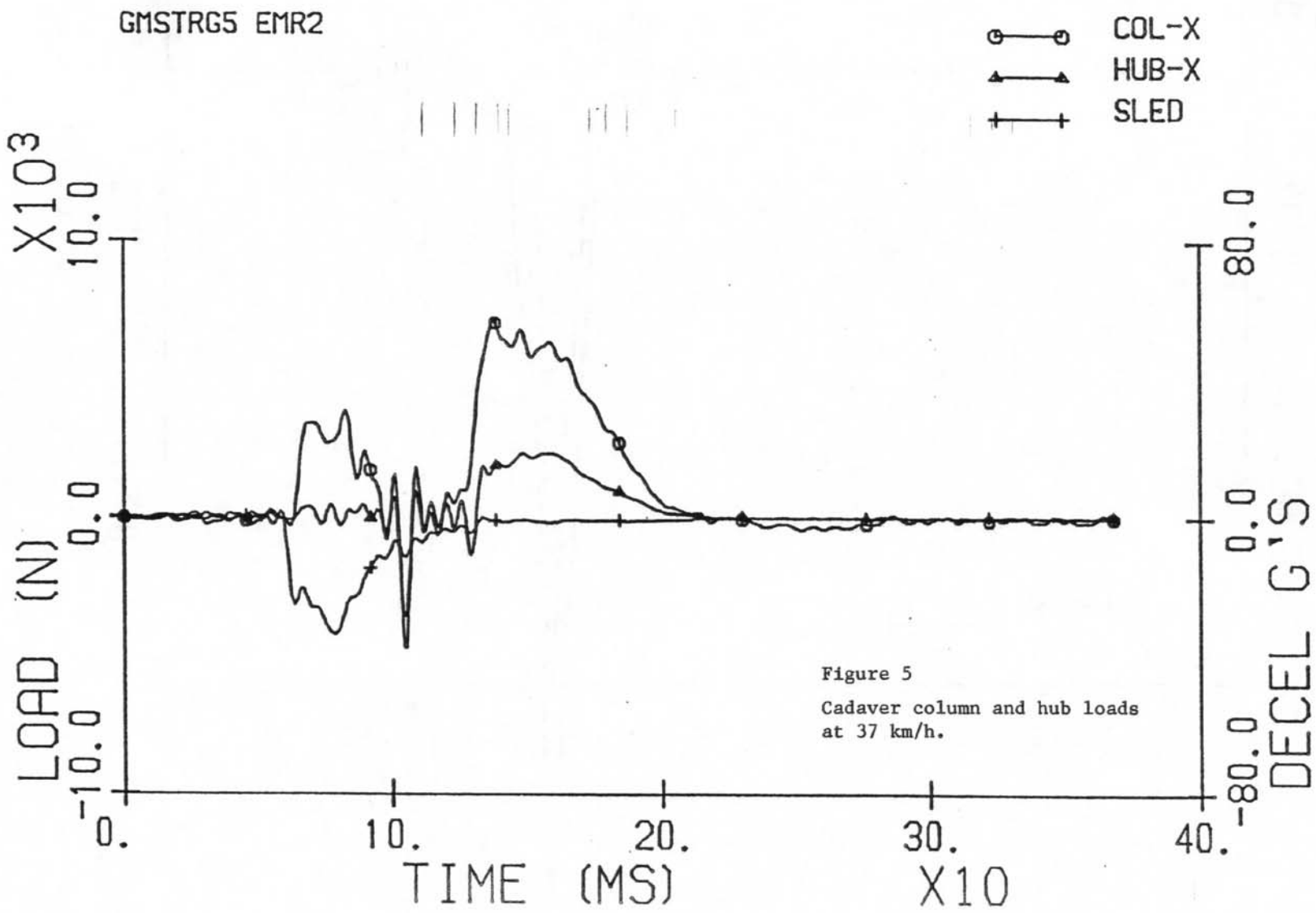

Figure 5

Cadaver column and hub loads at 37 km/h.

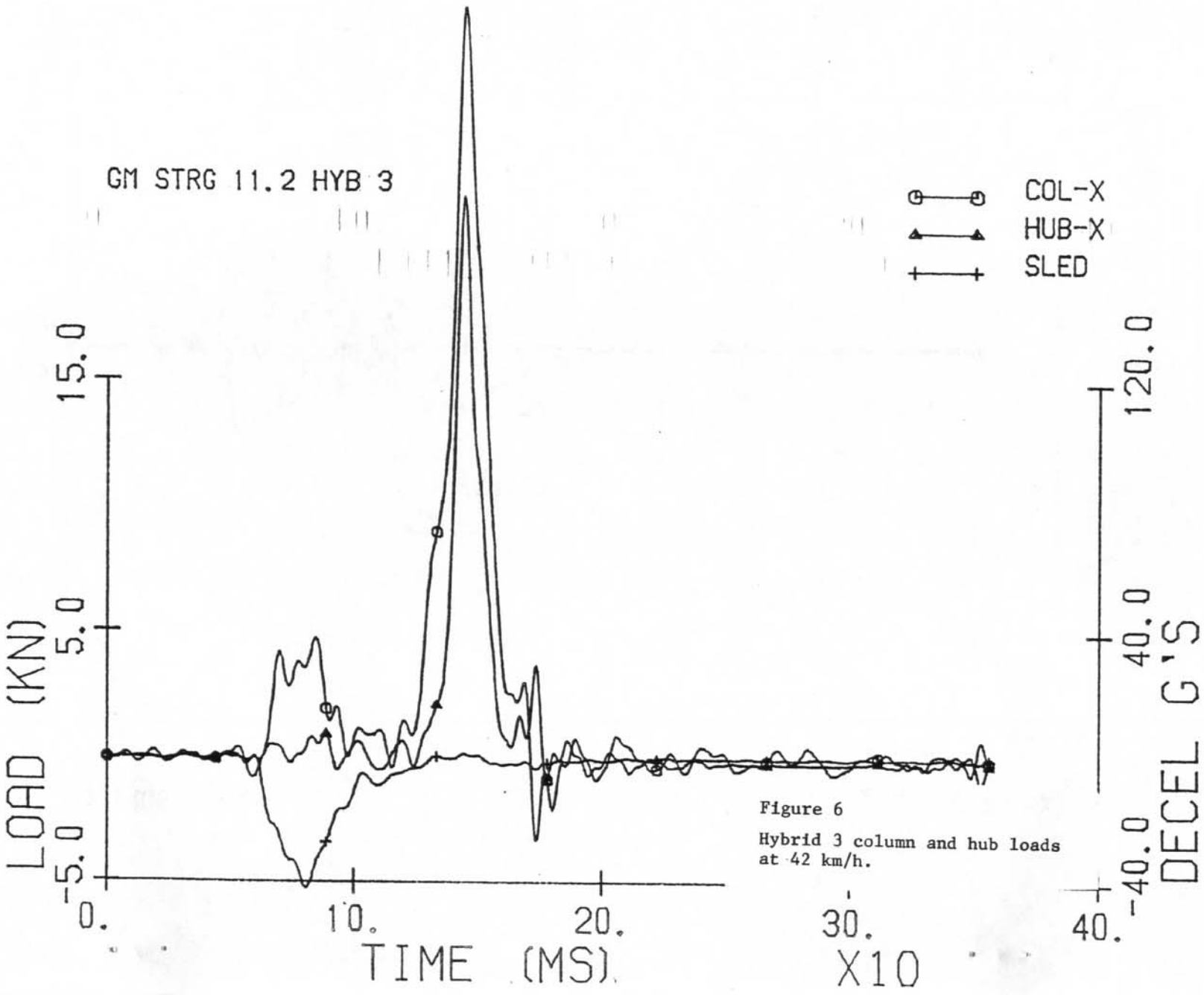

Figure 6

Hybrid 3 column and hub loads at 42 km/h.

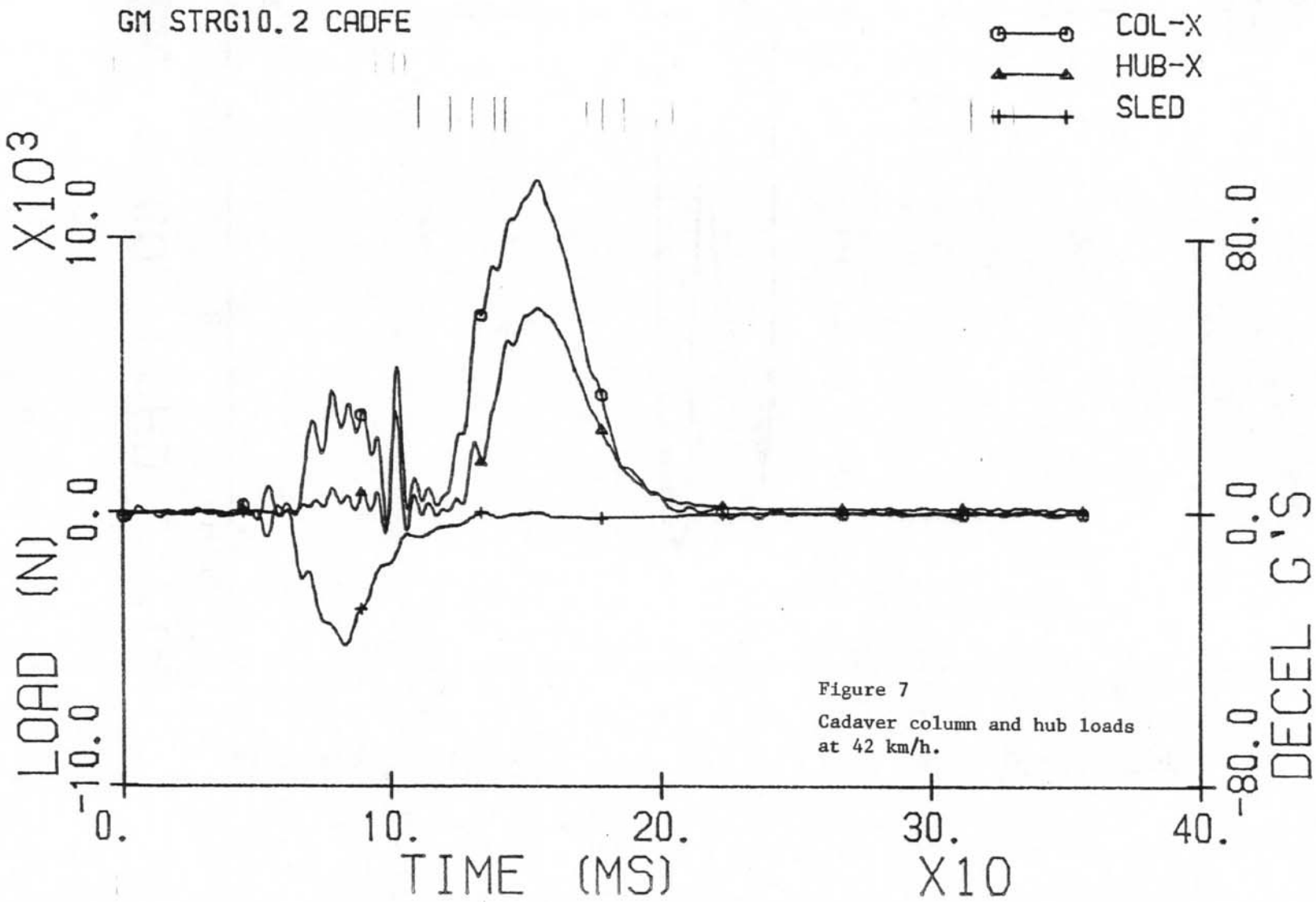

Figure 7

Cadaver column and hub loads at 42 km/h.

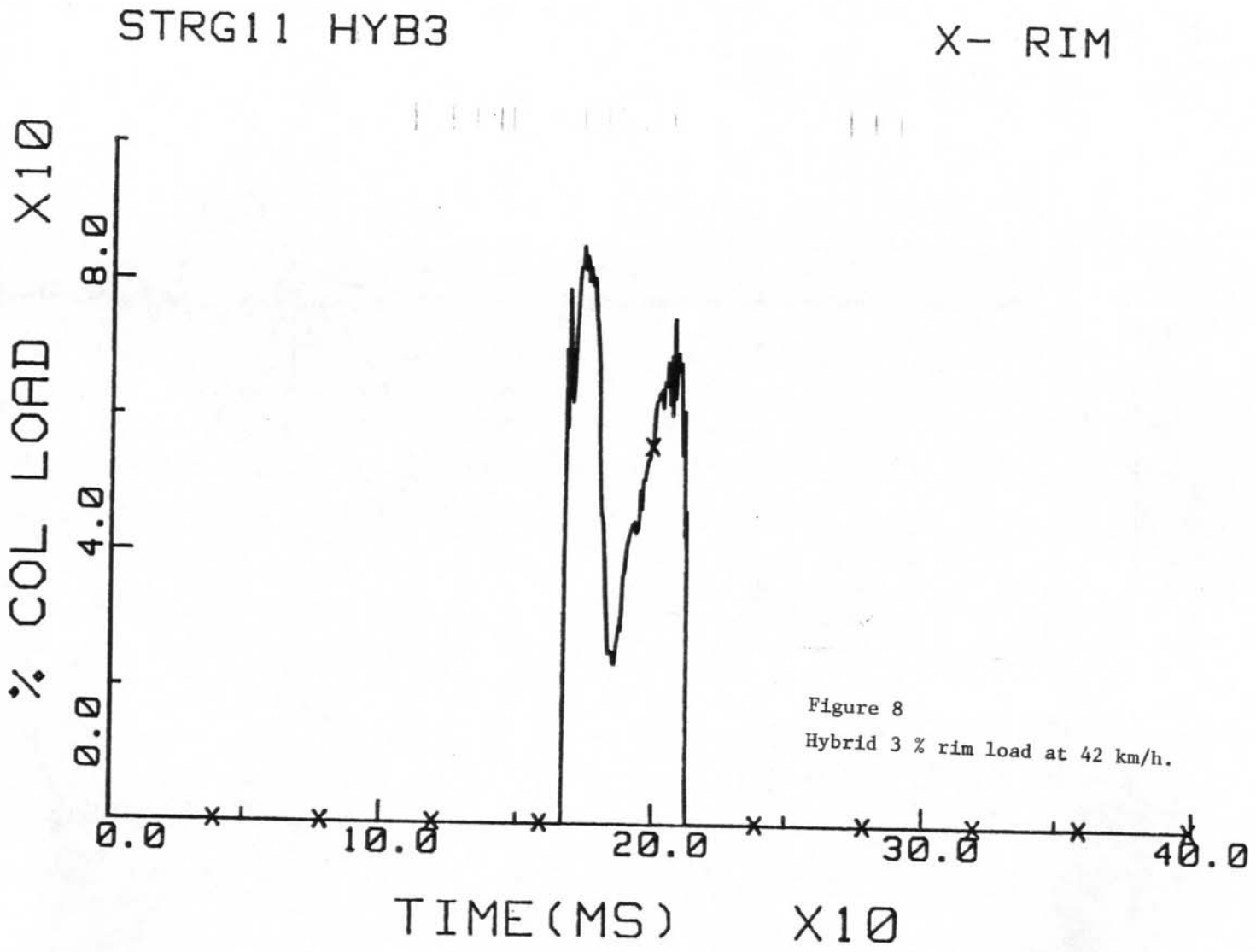

Figure 8
Hybrid 3 % rim load at 42 km/h.

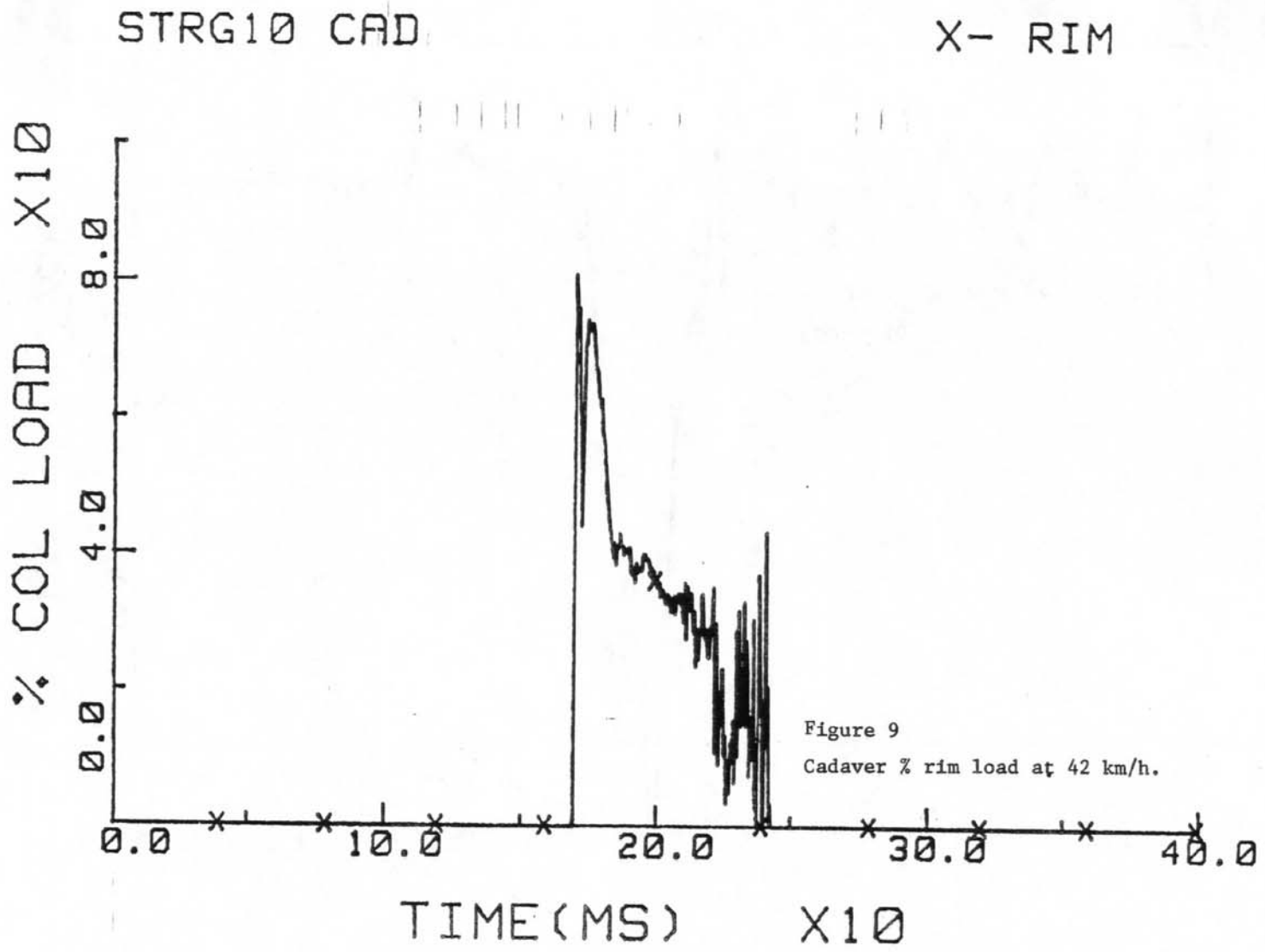

Figure 9
Cadaver % rim load at 42 km/h.

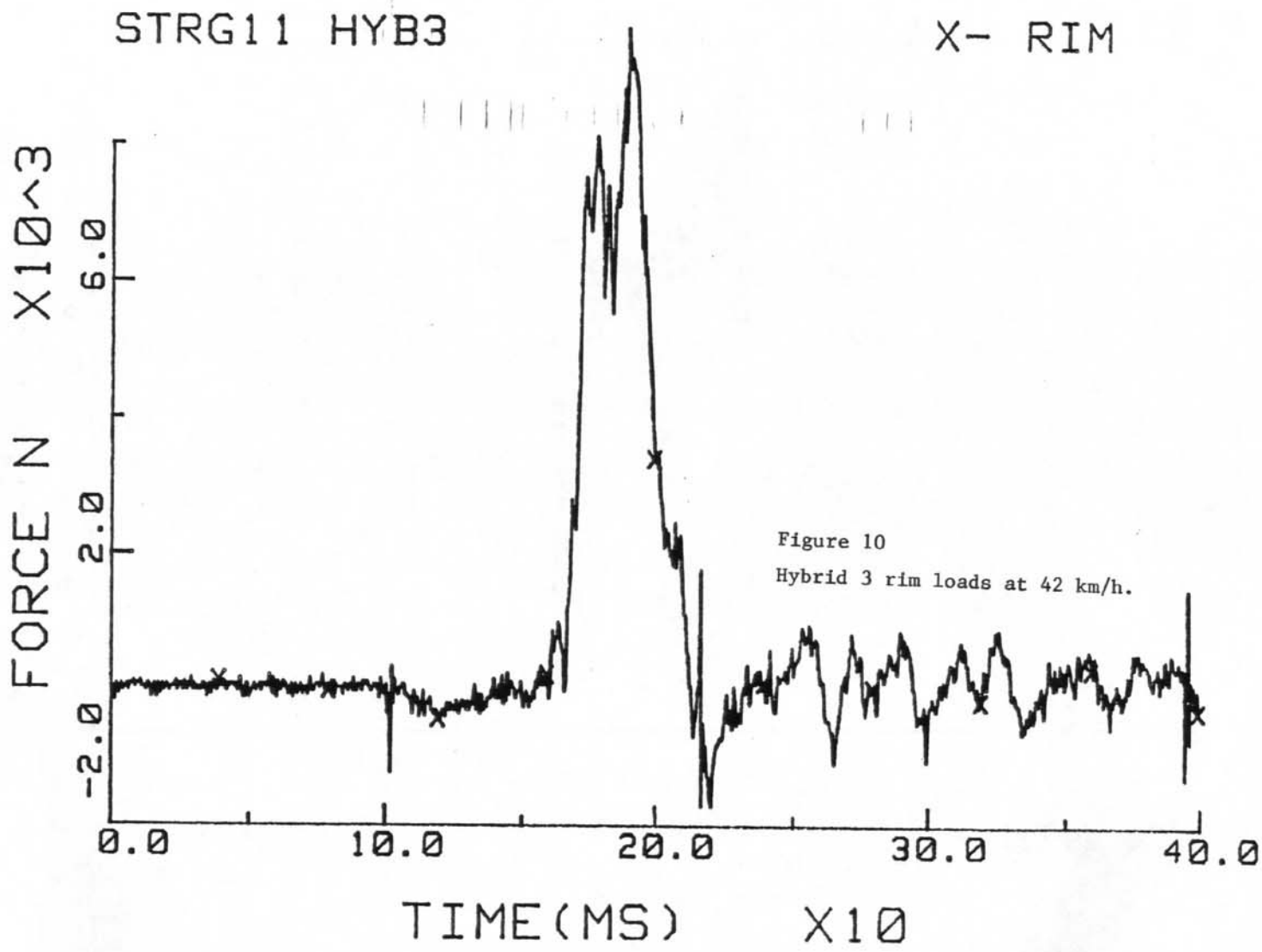

Figure 10
Hybrid 3 rim loads at 42 km/h.

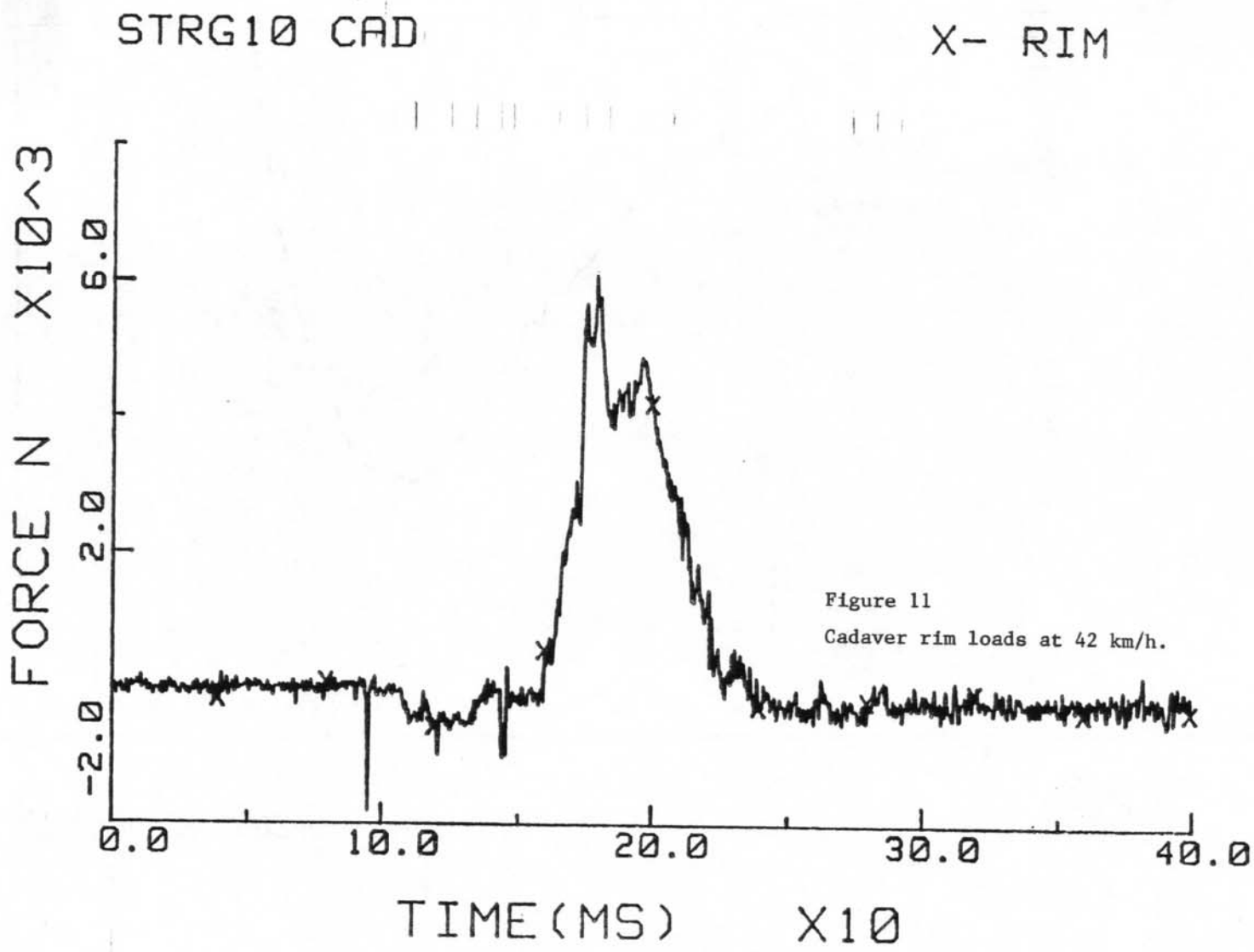

Figure 11
Cadaver rim loads at 42 km/h.

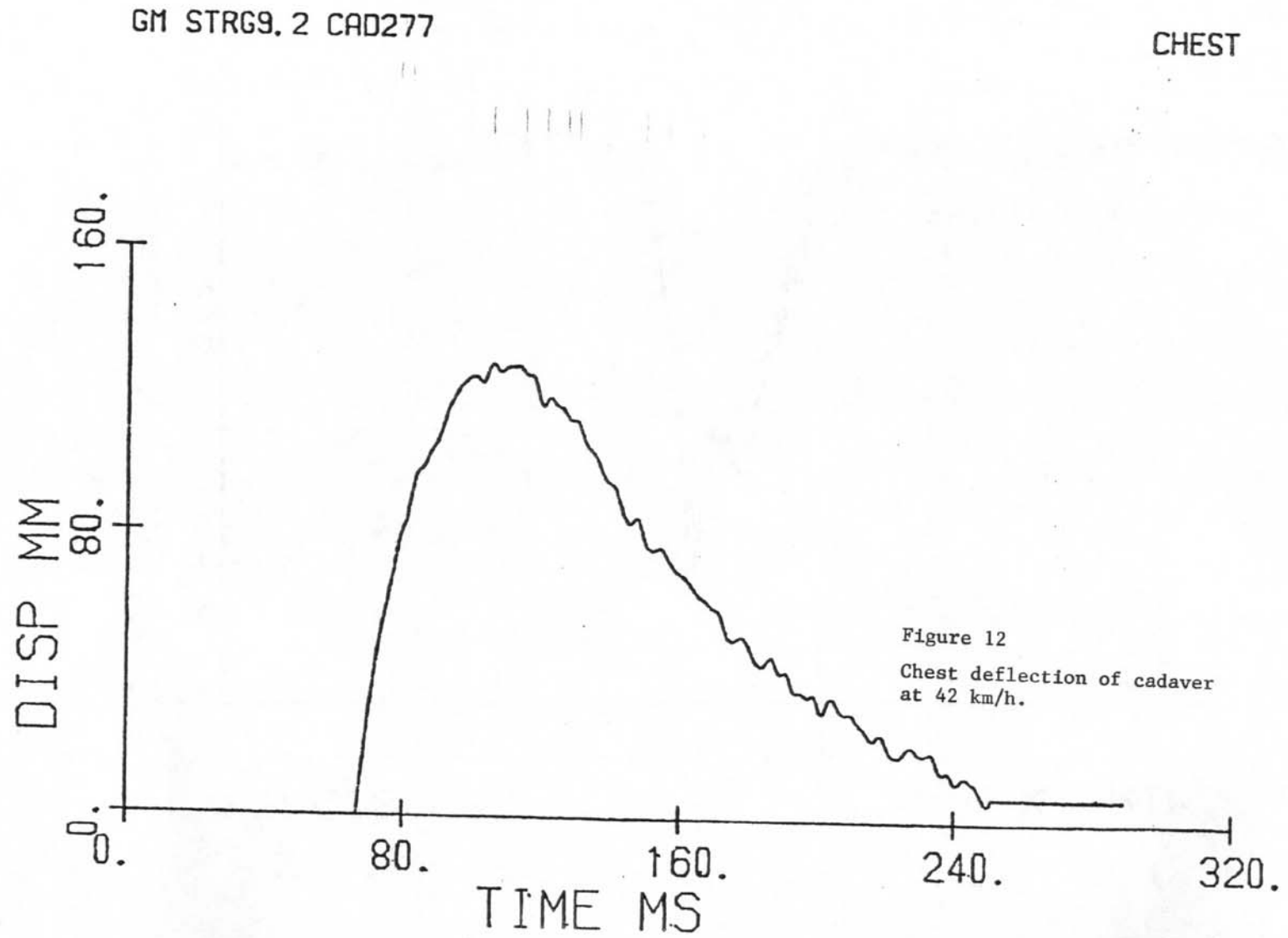

Figure 12

Chest deflection of cadaver at 42 km/h.

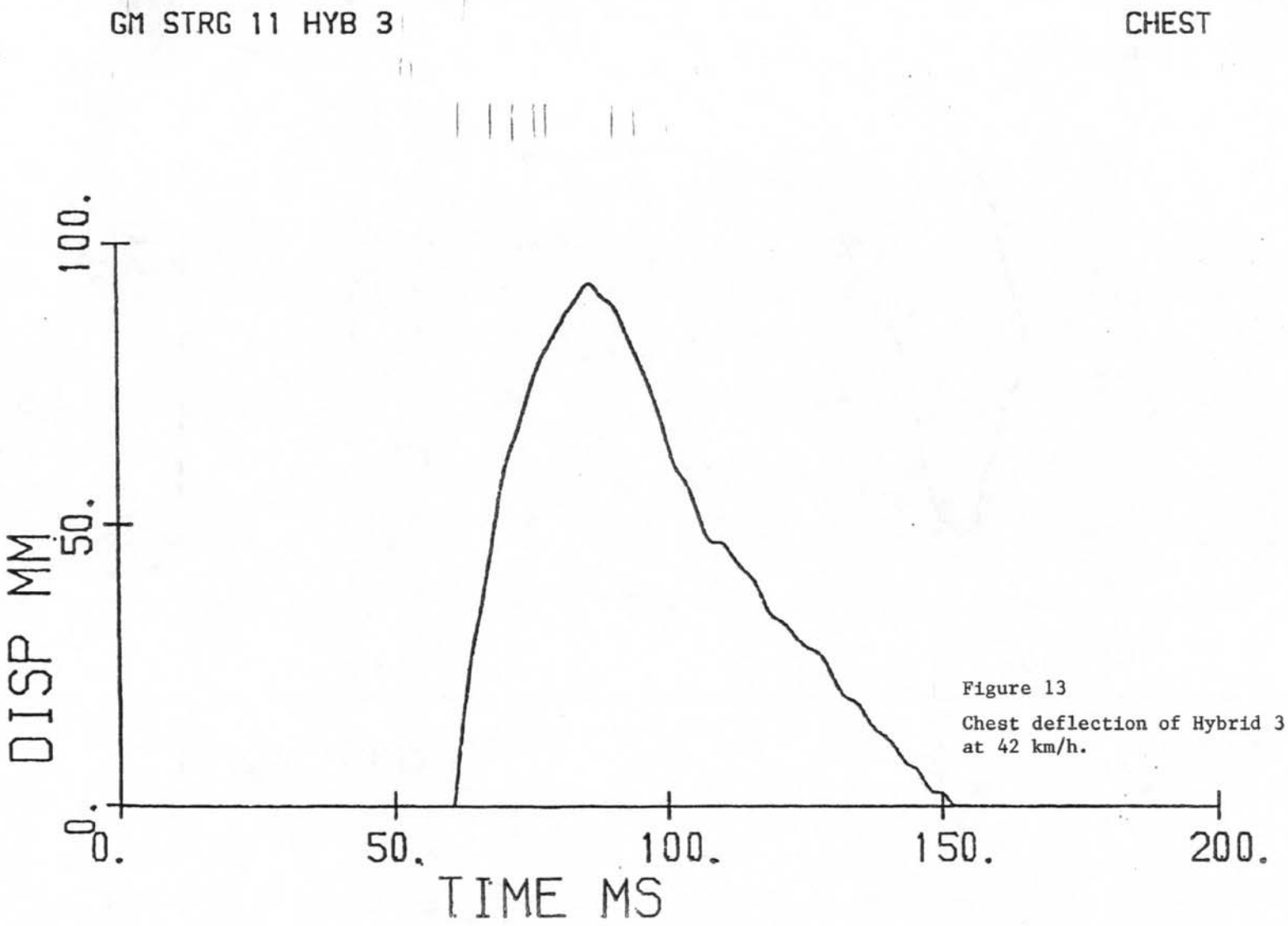

Figure 13

Chest deflection of Hybrid 3 at 42 km/h.

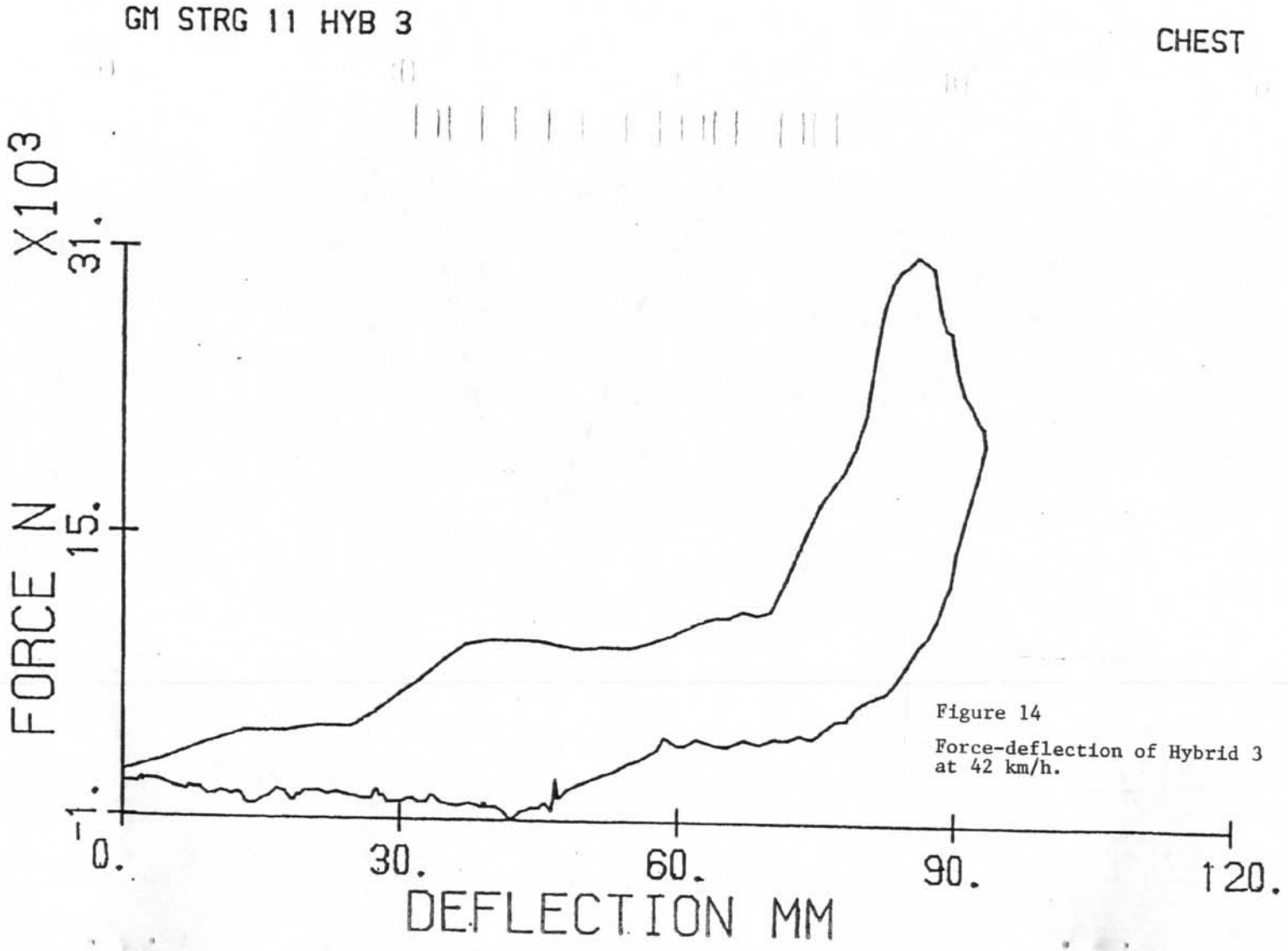

Figure 14

Force-deflection of Hybrid 3 at 42 km/h.

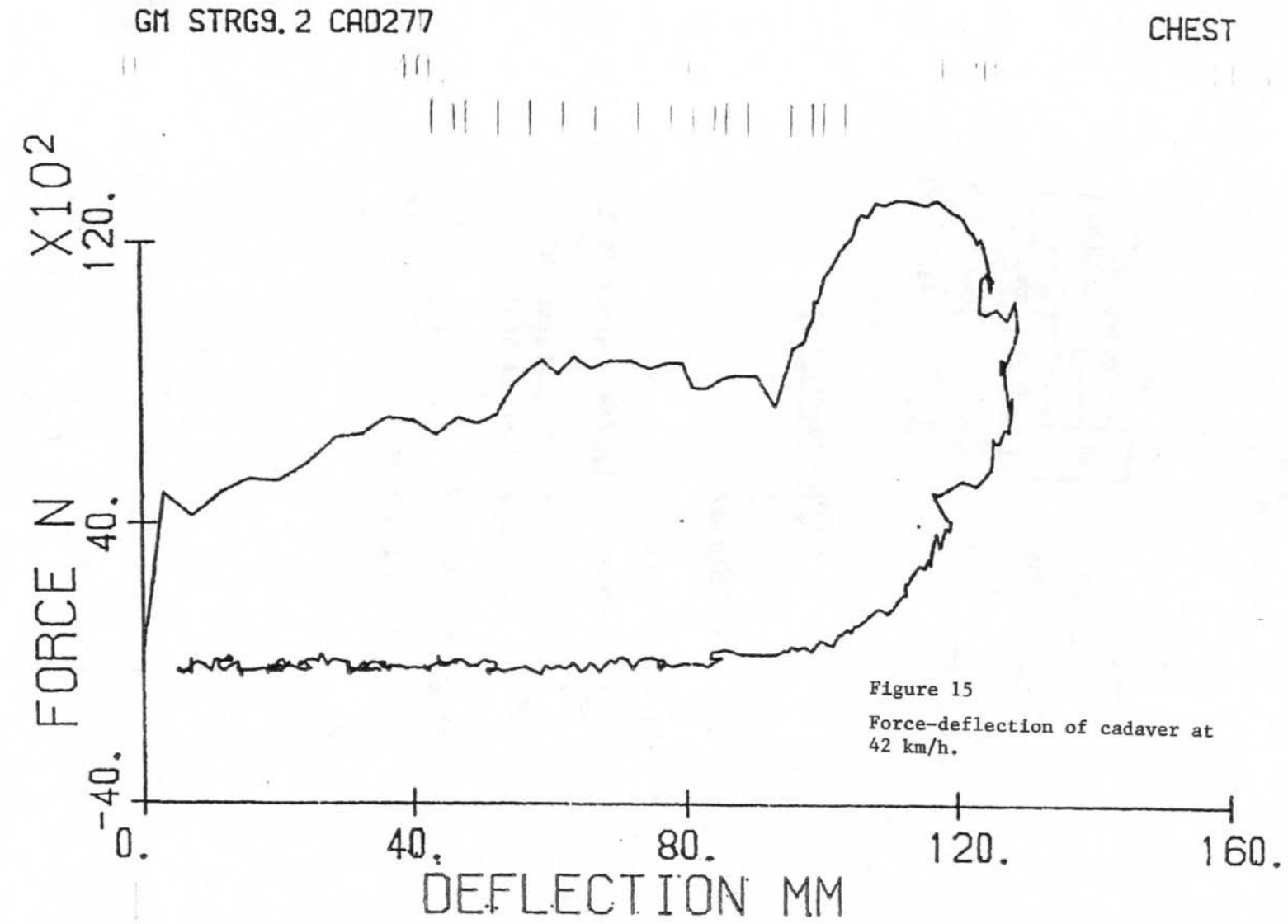

Figure 15

Force-deflection of cadaver at 42 km/h.

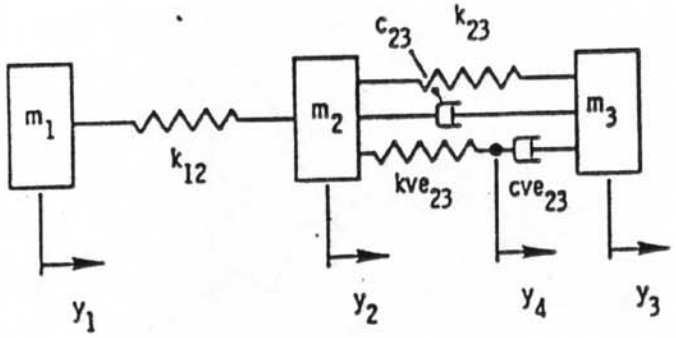

CADAVER PARAMETERS

K_{12} = 1600 LBS/IN

M_2 = .7 LBS

K_{23} = 60 OR 410 LBS/IN, CHANGE AT 1.3 IN.

C_{23} = 2.3 LBS/IN/SEC COMPRESSION
12.5 LBS/IN/SEC EXTENSION

KVE_{23} = 75 LBS/IN

CVE_{23} = 1.0 LBS/IN/SEC

M_3 = 40 LBS

Figure 16

Lobdell model with original cadaver parameters.

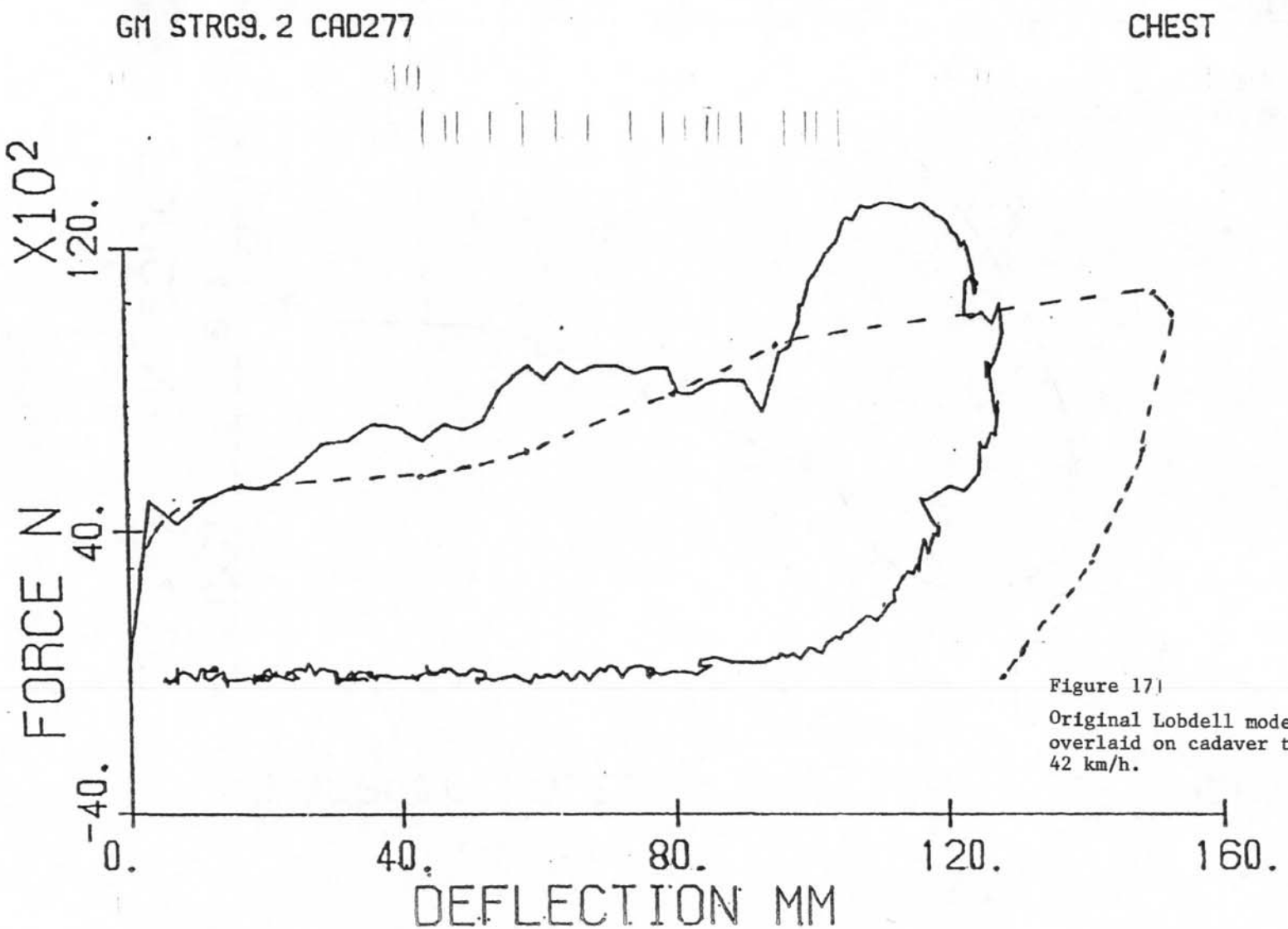

Figure 17

Original Lobdell model results overlaid on cadaver test results, 42 km/h.

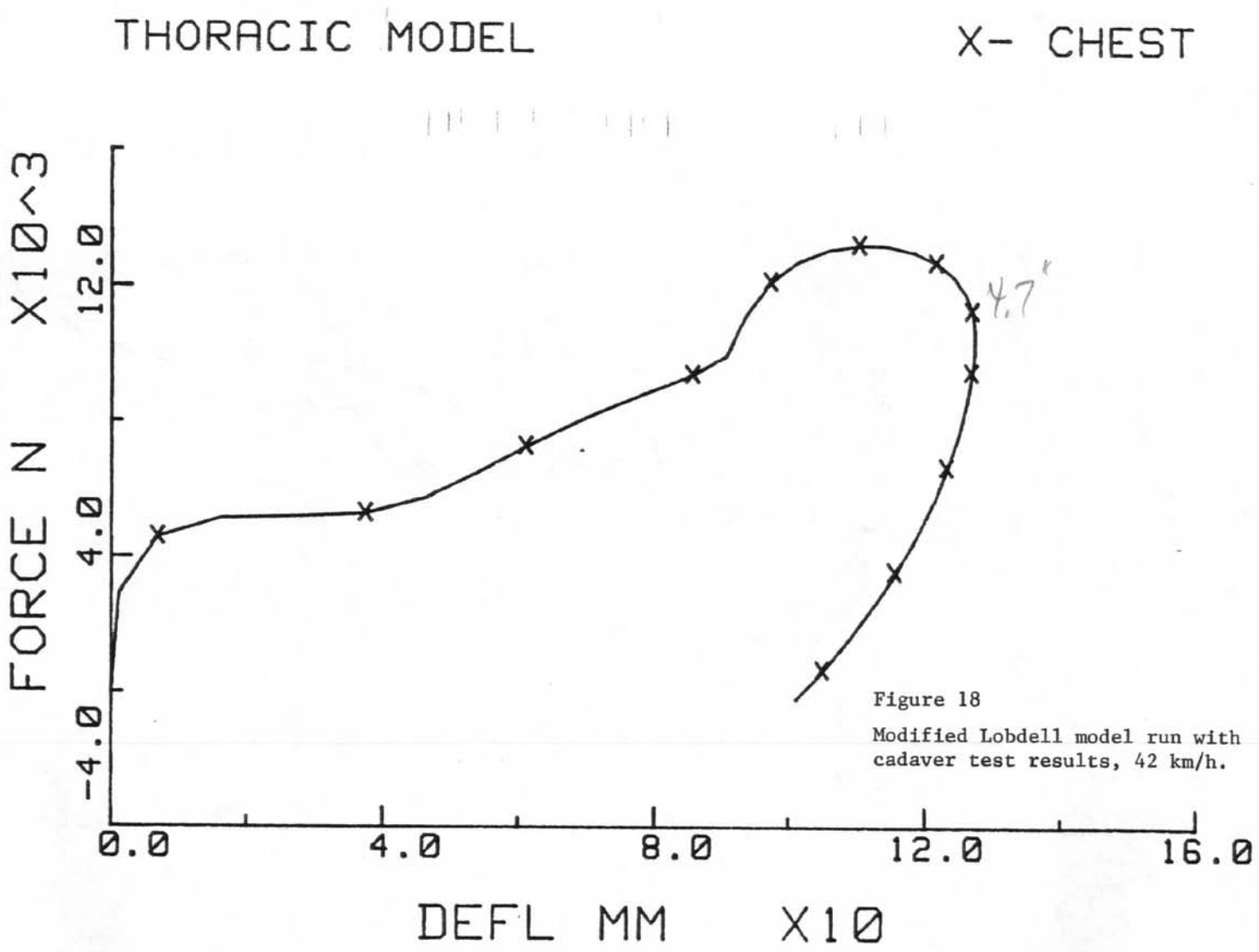

Figure 18

Modified Lobdell model run with cadaver test results, 42 km/h.

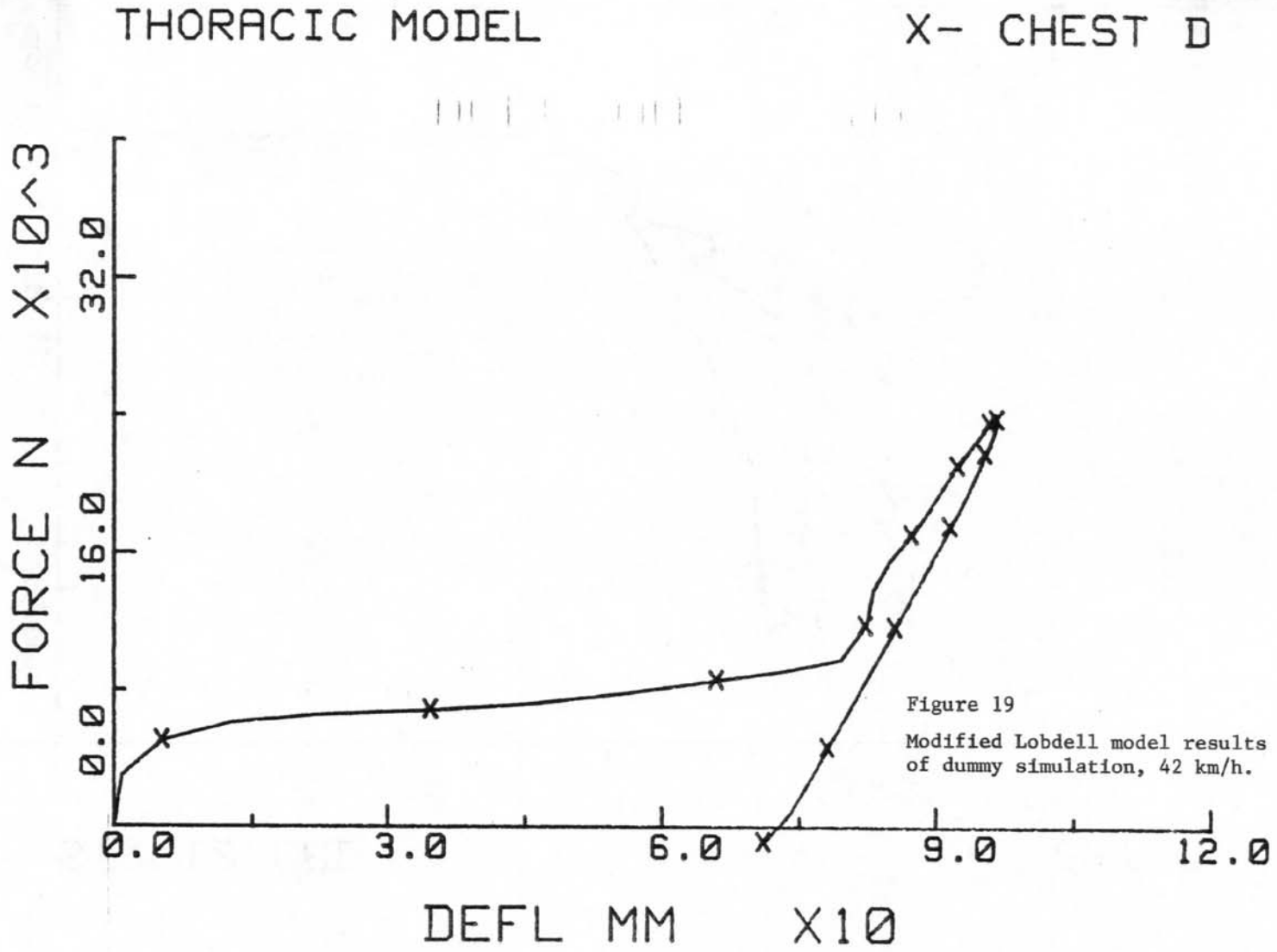

Figure 19

Modified Lobdell model results of dummy simulation, 42 km/h.

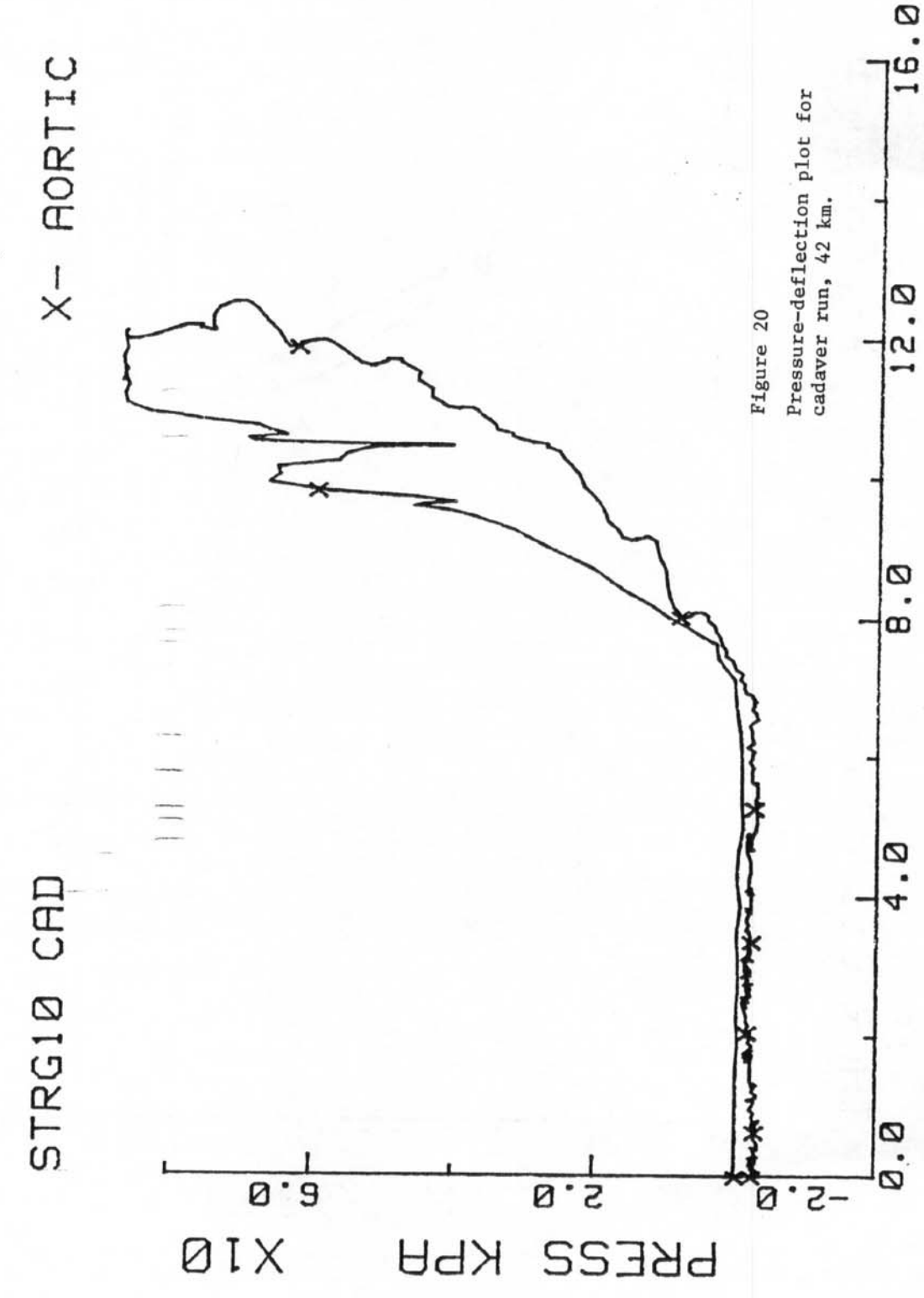

Figure 20
Pressure-deflection plot for cadaver run, 42 km.